Diverse States and Properties of Polymer Nanoparticles and Gel Formed by Polyethyleneimine and Aldehydes and Analytical Applications

ARTICLE *in* ANALYTICAL CHEMISTRY · AUGUST 2015

Impact Factor: 5.64 · DOI: 10.1021/acs.analchem.5b01138 · Source: PubMed

8 AUTHORS, INCLUDING:

Yu Ling

Southwest University in Chongqing

9 PUBLICATIONS **46** CITATIONS

SEE PROFILE

Zhong Feng Gao

Southwest University in Chongqing

20 PUBLICATIONS **84** CITATIONS

SEE PROFILE

analytical chemistry

Article

pubs.acs.org/ac

Diverse States and Properties of Polymer Nanoparticles and Gel Formed by Polyethyleneimine and Aldehydes and Analytical Applications

Yu Ling,[†] Fei Qu,[†] Qian Zhou,[†] Ting Li,[†] Zhong Feng Gao,[†] Jing Lei Lei,[‡] Nian Bing Li,*[,†] and Hong Qun Luo*[,†]

[†]Key Laboratory of Luminescent and Real-Time Analytical Chemistry, Ministry of Education, School of Chemistry and Chemical Engineering, Southwest University, Chongqing 400715, People's Republic of China

[‡]College of Chemistry and Chemical Engineering, Chongqing University, Chongqing 400044, People's Republic of China

Supporting Information

ABSTRACT: Multicolor polymer nanoparticles (or dots) were prepared via the reaction between hyperbranched polyethyleneimine (PEI) and aldehydes, and when the concentration of aldehydes was lower, the final mixture displayed gelation behavior. This phenomenon can be applied to visual detection of aldehydes. Moreover, the colors of the polymer dots and gel are varied by using different kinds of aldehydes, which can be utilized for visual discrimination of aldehydes. For simplicity, we focus our attention on the interaction between PEI and formaldehyde. The nanoparticles show an average diameter of 42 nm, emit bright cyan fluorescence with high quantum yield, and exhibit high water dispersibility and excellent photostability. Due to the advantages, our polymer nanoparticles (PNPs) are utilized as a fluorescent probe for imaging in living SK-N-SH cells. Furthermore, valuable explorations have been carried out on the fundamental properties of PNPs, such as concentration-dependent fluorescence, pH-dependent fluorescence, and solvent effect.

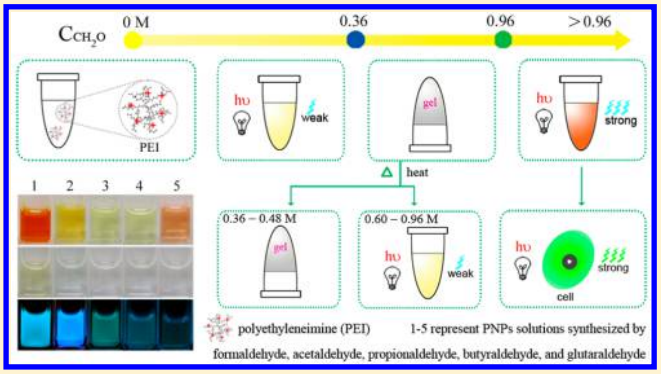

In most cases, the performance of a fluorescence technique is significantly dependent on the properties of the fluorophore, such as fluorescence brightness and photostability, which largely determine the sensitivity and reliability of the method.[1] Organic dyes, such as fluorescein, cyanine, and rhodamine, are versatile fluorophores applied in biological imaging and biosensors.[2] However, the limitations of traditional dyes, such as poor photostability and low absorptivity, have posed great difficulties for the further development of high-sensitivity imaging techniques and assays. Semiconductor quantum dots (Qdots) exhibit broad absorption bands and tunable, narrow emissions with improved brightness and photostability over conventional fluorescent dyes.[3−5] Nevertheless, Qdots are not bright enough and their toxicity is still a critical concern in biological applications. Various fluorescent dots were developed for biological applications, such as carbon dots[6,7] and silicon dots.[8,9] However, the surface modification of carbon dots or silicon dots is difficult. Conjugated polymers (CPs), which contain large conjugated backbones and delocalized electronic structure, have attracted considerable attention for both optoelectronic and biological applications. Generally, to fulfill biological applications, water-soluble CPs have been developed by modifying the side chains with charged moieties, and their applications in biological/chemical sensors, fluorescence imaging, and gene and drug delivery have been successfully realized.[10−18] However, several obstacles still exist, such as difficult conjugation processes and complicated separation and purification steps. In recent years, conjugated polymer nanoparticles (CPNs), also called conjugated polymer dots, have been successfully prepared and attracted considerable attention because of their outstanding properties, including high brightness, high quantum yield, excellent photostability, and low toxicity.[1,19−27] CPNs have demonstrated a wide range of applications such as fluorescence imaging, biosensing, drug/gene delivery, and material science fields.[21−26]

The photoluminescence originating from poly(amidoamine) (PAMAM) dendrimers was attributed to the formation of some fluorescent chemical species whose structures are still unidentified.[28,29] Although dendrimers have a more regular and well-defined structure, hyperbranched polymers or imperfect dendrimers, such as poly(amino ester)s,[30] display a more promising potential for applications due to their relatively simple synthesis.

Received: March 25, 2015
Accepted: August 3, 2015
Published: August 3, 2015

DOI: 10.1021/acs.analchem.5b01138
Anal. Chem. 2015, 87, 8679−8686

Polyethyleneimine (PEI), a water-soluble cationic polymer that contains a large number of amino groups with a three-dimensional network structure, has been used for a wide variety of biological applications.[31,32] Meanwhile, a few reports have described the fluorescent properties and applications of PEI. In previous literature,[33] hyperbranched PEI exhibited weak blue emission and its linear analogue is capable of producing strong photoluminescence by oxidation. It was reported that ethylenediamine and a secondary amine in the molecule (such as PEI, peptides, proteins, and so on) were key components for the especially high autofluorescence of glutaraldehyde.[34] Recently, fluorescent organic nanoparticles were prepared via hydrothermal treatment (100 °C, 2 h) of maltose and polyethyleneimine in water.[35] In this work, multicolor polymer nanoparticles (PNPs) and gel were prepared via the reaction between PEI and aldehydes. The fundamental properties of PNPs have been investigated, and a possible mechanism has been proposed. Besides glutaraldehyde, other aldehydes, such as formaldehyde, could also cause strong fluorescence. PEI has been widely used as a gene delivery vehicle both in vitro and in vivo.[31,32] In this regard, amine-terminated PEI forms PNPs that demonstrate great potential for bioconjugation.

EXPERIMENTAL SECTION

Chemicals. Polyethyleneimine (PEI, M_w = 10 000, 99%), formaldehyde (35 wt %, 12 M), acetaldehyde (99 wt %, 17 M), propionaldehyde (97 wt %, 13 M), butyraldehyde (98 wt %, 11 M), glutaraldehyde (50 wt %, 5 M), and formic acid (88 wt %, 23 M) were purchased from Aladdin Ltd., Shanghai, China. All other chemicals not mentioned here were of analytical reagent grade and were used as received. Ultrapure water (18.2 MΩ·cm) was used throughout the experiments.

Apparatus. A Hitachi F-4500 spectrofluorophotometer (Tokyo, Japan), equipped with a 150-W xenon lamp, was used for recording the fluorescence spectra. UV/vis absorption spectra were recorded on a UV−vis 2450 spectrophotometer (Shimadzu). Transmission electron microscopy (TEM) measurements were performed with a JEM 1200EX transmission electron microscope at an accelerating voltage of 120 kV. Dynamic light scattering (DLS) measurements were carried out on a Zetasizer Nano-ZS90 (Malvern, U.K.) instrument. Nuclear magnetic resonance (NMR) spectra were collected on an Avance III 600 (600 MHz). Fourier transform infrared (FT-IR) spectra were obtained on a Bruker IFS 113v spectrometer after the fine powder was pelleted with KBr. A rapid mixing device (Ronghua Instrument Plant, Jiangsu, China) was used to mix solutions completely. The pH values of solutions were measured with a pH meter (PHS-3C, Shanghai Leici Instrument Co., Ltd.).

Synthesis of Polymer Nanoparticles. Typically, the PEI solution (20 mM) was prepared by dissolving 0.2 g of PEI in 1.0 mL of ultrapure water. The concentration of PEI is calculated in terms of M_w. PEI solution (40 μL) was added to water (10 μL). Next, an aldehyde (50 μL) was added and the solution was mixed well under vigorous stirring. The final solution (100 μL) was then heated at 95 °C for 25 min. The as-prepared PNP solution was stable for at least 2 months. For further use, the PNP solution was diluted with ultrapure water.

Synthesis of Gel. PEI solution (20 mM, 30 μL) was added to water (66 μL) in a 0.5 mL eppendorf tube. An aldehyde (4 μL) was then added and the solution (100 μL) was mixed well under vigorous stirring.

RESULTS AND DISCUSSION

In order to synthesize multicolor PNPs and gel in one simple step, we investigated the interaction between PEI and aldehydes. The PEI solutions show weak fluorescence, gelation, and strong fluorescence upon adding 0.12−0.36 M, 0.36−0.96 M, and more than 0.96 M formaldehyde, respectively (Scheme 1). Differently from previous literature,[36,37] in this work not only have PNPs been synthesized but also gelation behavior has been observed when the concentration of aldehydes is lower. This phenomenon can be applied to visual detection of aldehydes. Similarly, other aldehydes such as acetaldehyde, propionaldehyde, butyraldehyde, and glutaraldehyde can also react with PEI to generate multicolor PNPs and gel. Moreover, the colors of the polymer dots and gel are varied by using different kinds of aldehydes, which may provide an inspiring strategy for naked-eye discrimination of aldehydes. In contrast, no fluorescence signal is detected for PEI or aldehydes alone. For simplicity, we focus our discussion on the interaction between PEI and formaldehyde. Excitation, emission, and absorption spectra of PNPs formed by PEI and formaldehyde are shown in Figure 1. The PNP solution has a characteristic absorption band at 335 nm, while PEI and formaldehyde alone have nearly no absorption above 260 nm. The emission spectra of CPNs were observed with different excitation wavelengths

Scheme 1. Schematic Illustration of Diverse States of Polymer Nanoparticles or Gels Formed by PEI and Formaldehyde[a]

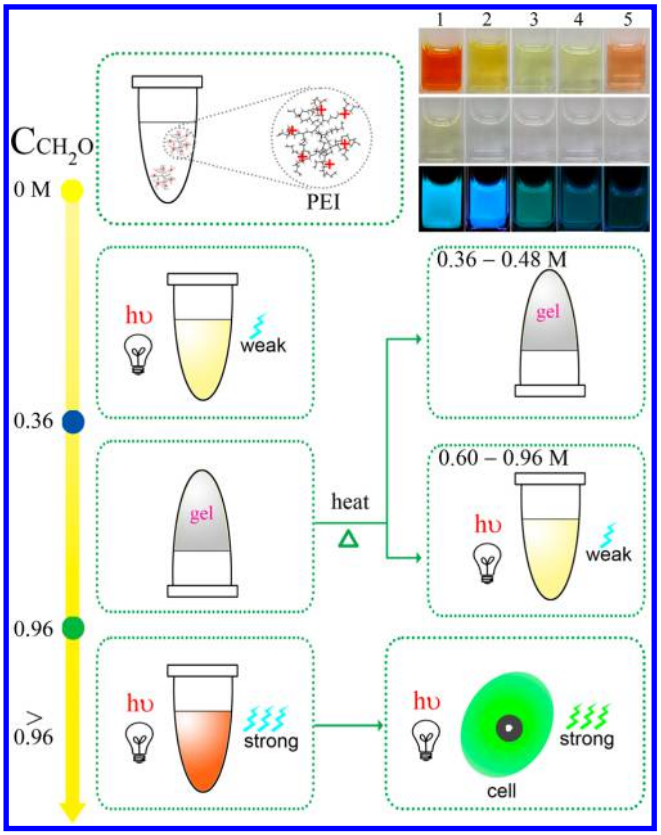

[a]The photographs show different diluted PNP solutions under visible light and UV lamp, in which 1, 2, 3, 4, and 5 represent the PNP solutions formed by the reaction of PEI with formaldehyde, acetaldehyde, propionaldehyde, butyraldehyde, and glutaraldehyde, respectively.

DOI: 10.1021/acs.analchem.5b01138
Anal. Chem. 2015, 87, 8679−8686

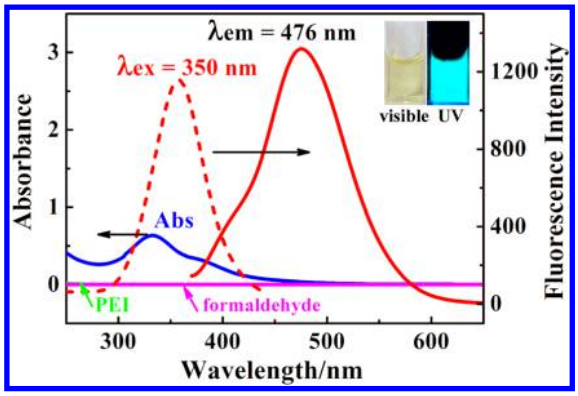

Figure 1. Excitation and emission spectra of PNPs (0.3% v/v) and absorption spectra of PNPs (0.3% v/v), PEI (80 μM), and formaldehyde (60 mM). (Inset) Photos of diluted PNP solution under visible light (left) and UV lamp (right, 365 nm).

from 320 to 370 nm and are shown in Figure S1. The TEM image with uranyl acetate staining (Figure 2) reveals that the as-

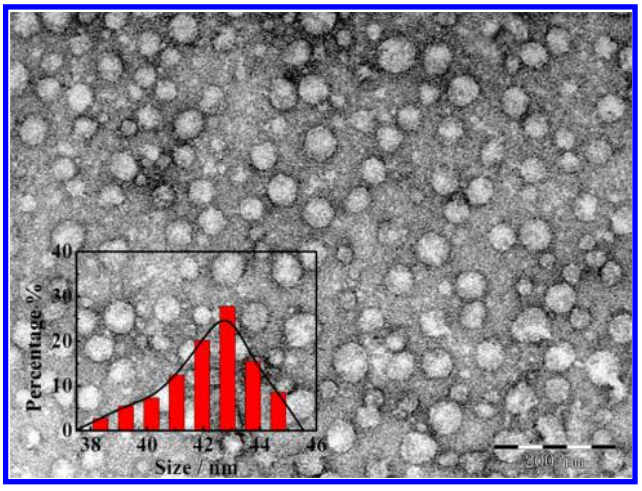

Figure 2. TEM image of PNPs. (Inset) Size distribution graph. The nanoparticles were stained with uranyl acetate.

prepared PNPs are nanoparticles of near-spherical morphology with an average diameter of 42 nm. The size of the PNPs is not very uniform and in fact ranges from 38 to 45 nm. Generally, excitation-dependent fluorescence behavior may result from different sizes of particles and surface defects.[38] The average size of the hydrodynamic diameter of PNPs measured by DLS analysis is 63 nm, which is larger than the TEM diameter (42 nm). This is because DLS gives the hydrodynamic diameter, whereas TEM gives the size of dry particles. The larger hydrodynamic diameter is due to hydration effects present in aqueous solution. Besides, polymer chains surrounding the core would be in a swollen state. The maximum excitation and emission wavelengths were detected to be 350 and 476 nm, respectively (Figure 1). In the inset of Figure 1, the diluted PNP solution shows slightly yellow under visible light, while it emits bright cyan fluorescence under a UV lamp. The quantum yield (QY) was calculated to be 45% by use of quinine sulfate as a reference, which is much higher than those of other fluorophores obtained from PEI.[33−35]

Figure 3 shows emission spectra of PNPs in different solvents, including methanol, ethanol, *n*-propanol, 2-propanol, 1-butanol, ethylene glycol (EG), *N*,*N*-dimethylformamide (DMF), acetonitrile, dimethyl sulfoxide (DMSO), tetrahydrofuran (THF), 1,4-dioxane, and ethylene glycol monomethyl ether (EGME). The emission peaks of PNPs in organic solvents exhibit a slight blue shift compared with that in water, and the fluorescence intensities increase except for those in methanol, acetonitrile, and 1,4-dioxane. The dipolar change and the decrease in solubility of PEI lead to collapse of the branches, which can directly influence the density of functional groups on the surface of PNPs and increase the interchain interactions. Because the formation of PNPs is driven by the folding and torsion of the polymer backbone, the density of functional groups on the particle surface plays a significant role in the performance of nanoparticles. The similar principle has been used to explain the behavior of poly[(9,9-dioctylfluorenyl-2,7-diyl)-*co*-(1,4-benzo-{2,1′,3}-thiadazole)] (PFBT) dots.[39] However, the characteristic absorption was insensitive to solvent effects. In other words, the dipolar change induced by solvents actually influences the excited state rather than the ground state of the fluorophore. In addition, the fluorescence intensity of PNPs in 1,4-dioxane decreased obviously with time (see Figure 3C), and the characteristic absorption band (335 nm) disappeared (see Figure 3D). This result indicates that the ground state of the fluorophore is also changed. In THF the fluorescence intensity of PNPs is enhanced with time (Figure 3E), the absorption shoulder peak at 250−300 nm displays an obvious blue shift, and the absorbance increases with time (Figure 3F). This result suggests that intramolecular charge transfer (ICT) has occurred.[40,41] The fluorescence intensity of the PNPs was found to be pH-dependent (Figure 4A). The pH values of the solutions were adjusted with Britton−Robinson (BR) buffers from pH 1.81 to 11.98. The PNPs show high fluorescence intensity at low pH values, and the fluorescence intensity decreases slightly from pH 1.81 to 11.98. Moreover, the fluorescence intensity exhibits two linear relationships over the pH ranges 1.81−7.54 and 7.54−11.98 (Figure 4B). The pH-dependent property of the PNPs may be attributed to not only the charge distribution of different amine groups of PEI but also the change in chain conformation with the local structure of the polymer.[42] The pH-dependent fluorescence of PNPs could be utilized to determine pH in a wide range. PEI contains a large number of primary, secondary, and tertiary amino groups.[43] The primary amino groups can interact with aldehyde to form a Schiff base. However, aliphatic substituted imine is unstable. On the other hand, formaldehyde is readily oxidized to formic acid. To clarify this hypothesis, formic acid (12.5 M) was mixed with PEI solution (8 mM) and water (10 μL). Then the final solution was heated at 95 °C for 25 min. After heating, the solution was slightly yellow. The values of emission wavelength were constant, which indicated formic acid interacted with PEI to form PNPs. Nevertheless, the fluorescence intensity decreased (Figure S2). It is possible that formaldehyde is conducive to the cross-linked reaction. This inference was confirmed by further measurements. From FT-IR spectra (Figure 5), the formation of amide can be observed. PEI (curve a) has characteristic absorption bands at 3294, 2921, and 1123 cm^{-1} corresponding to the stretching vibrations of N−H, CH_2, and C−N bonds, respectively.[44] Curves b, c, and d represent the FT-IR spectra of PNPs, gel at room temperature, and gel after heating, respectively. The fact that curves b−d are similar indicates that PNPs and gel before and after heating have similar structures. Moreover, a new sharp peak at 1650 cm^{-1} (curves b−d) can be attributed to amide linkage (-CONH-) and the one at 3442 cm^{-1} is associated with

DOI: 10.1021/acs.analchem.5b01138
Anal. Chem. 2015, 87, 8679−8686

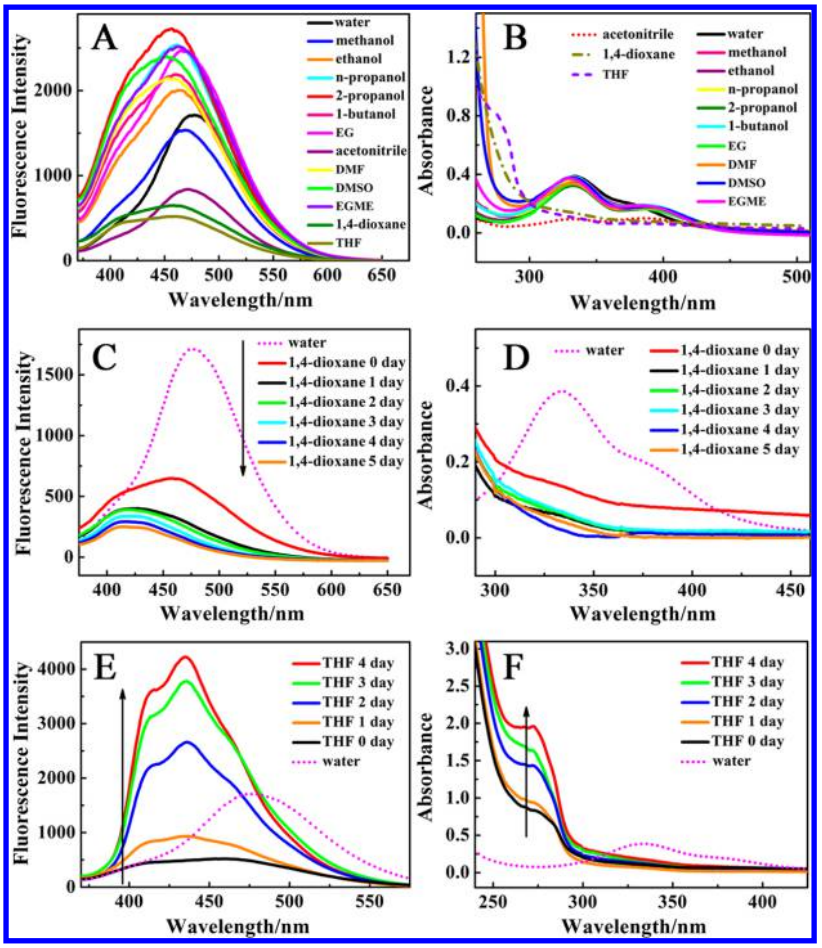

Figure 3. (A) Emission and (B) absorption spectra of PNPs (0.3% v/v) in different solvents; (C) emission and (D) absorption spectra of PNPs in THF; and (E) emission and (F) absorption spectra of PNPs in 1,4-dioxane.

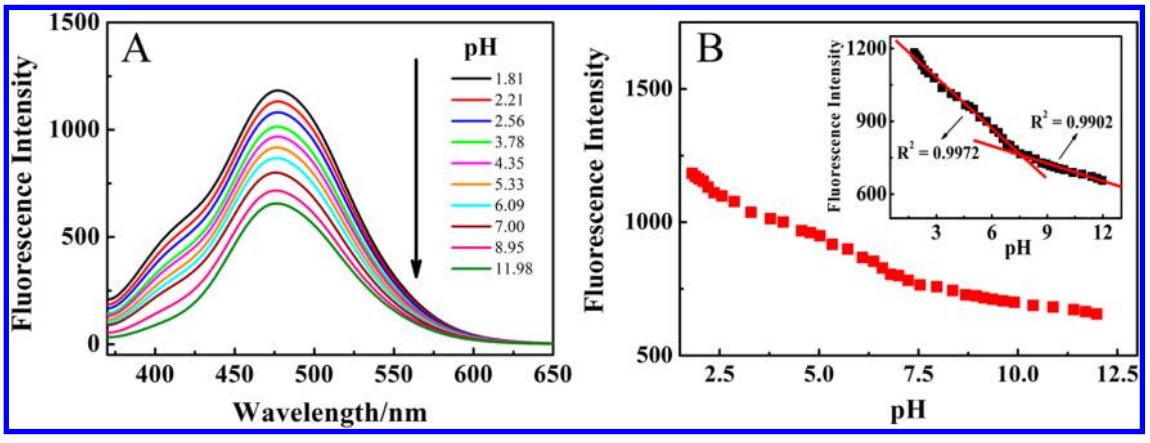

Figure 4. (A) Emission spectra of PNPs (0.3% v/v) in Britton–Robinson (BR) buffer solutions from pH 1.81 to 11.98. (B) Relationship between pH value and fluorescence intensity. (Inset) The two linear pH ranges are 1.81–7.54 and 7.54–11.98.

secondary amines.[44,45] The peaks at 3213 and 1400 cm^{-1} correspond to hydroxyl groups, and the peak at 1100 cm^{-1} is associated with the stretching vibration of O–H.[46] The PNP solution was evaporated, yielding a yellow powder. The product was then dissolved in D_2O. ^1H NMR (D_2O, 600 MHz, Figure S3): δ = 8.45 (s, -CONH-). This result further proved the formation of amide linkage (-CONH-). The PNPs formed by hyperbranched PEI have several structural features similar to the fluorescent chemical species formed by PAMAM,[28,29] such as abundant terminal groups and coexistence of tertiary amines and carbonyl groups.[30] Similarly, the PNPs reported here can emit fluorescence.

The experimental conditions for producing the PNPs have been optimized carefully. All the volumes of the final mixtures were 100 μL. At first, the concentration of PEI was fixed at 6 mM and the molar concentration of formaldehyde was optimized. As can be observed in Figure 6A, the fluorescence intensities increased with increasing concentration of formaldehyde and remained constant at a concentration over 6 M. Excess formaldehyde has little influence on the fluorescence

DOI: 10.1021/acs.analchem.5b01138
Anal. Chem. 2015, 87, 8679–8686

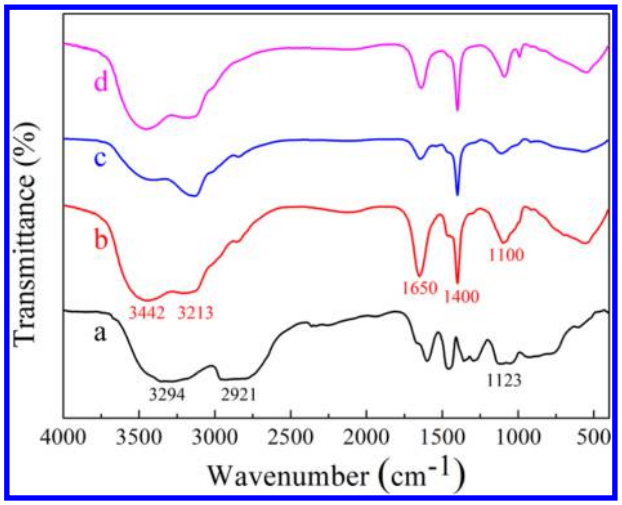

Figure 5. FT-IR spectra of (a) PEI, (b) PNPs, (c) gel before heating, and (d) gel after heating.

intensity. Correspondingly, the color of the diluted PNP solutions changed from nearly colorless to slight yellow and deepened with increasing concentration of formaldehyde (Figure 6E). Interestingly, the fluorescent color also depended on the concentration of formaldehyde (Figure 6F). To further investigate the molar radio of PEI to formaldehyde, the concentration of formaldehyde was fixed at 6 M and the concentration of PEI was studied. The fluorescence intensity kept stable at a concentration over 8 mM (Figure 6B). So the amounts of PEI (8 mM) and formaldehyde (6 M) were chosen as described in the Experimental Section. At room temperature (25 °C), the mixture of PEI and formaldehyde can change from colorless to slightly yellow very slowly and emit weak fluorescence. In the range 75−95 °C, higher temperature can accelerate the reaction obviously (Figure 6C). Considering that the boiling point of water is 100 °C, we chose 95 °C as the optimum temperature. After reaction at 95 °C for 25 min, the fluorescence intensity of the system almost keeps constant (Figure 6D). It is possible that higher temperature can accelerate the oxidation of formaldehyde to formic acid, which is a key factor to form amide. In addition, the molecular weight of PEI had an insignificant influence on fluorescence emission. When PEI of different molecular weights was used (M_w = 600, 1800, 10 000, and 70 000), the fluorescence intensity increased slightly, and the values of emission wavelength were constant (Figure S4).

From the relationship between fluorescence intensity and concentration of the PNPs (Figure 7), it can be seen that

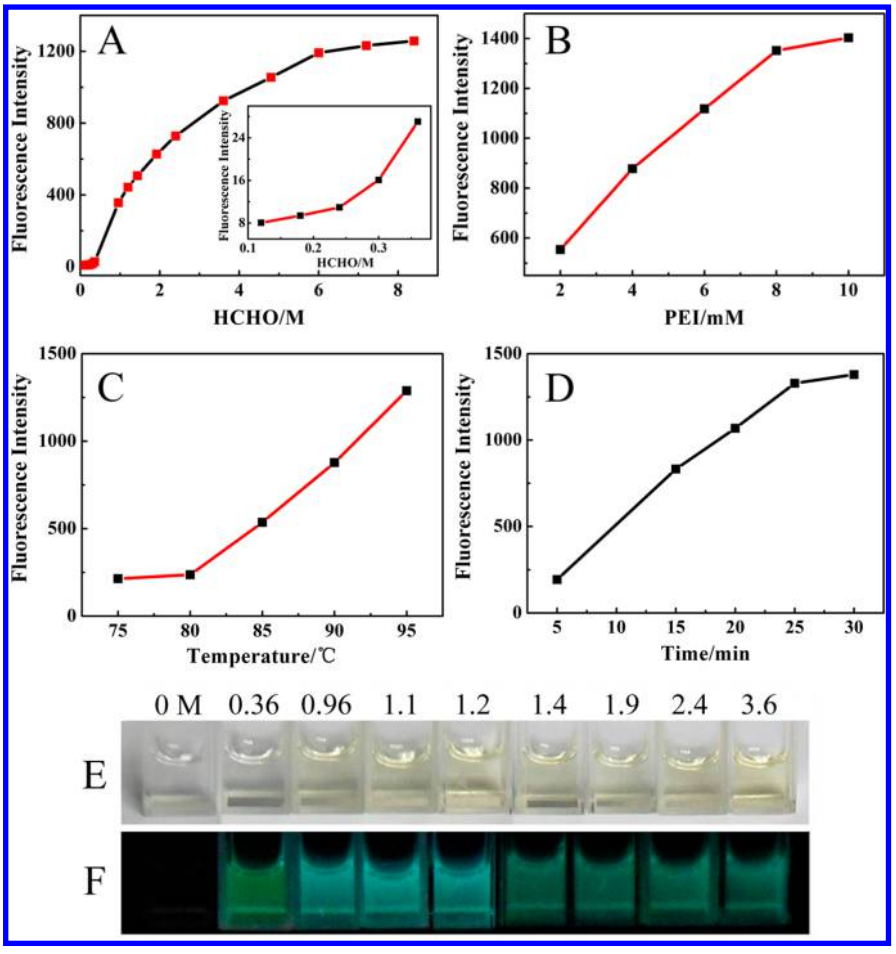

Figure 6. (A) Effect of formaldehyde concentration on fluorescence intensity. The concentration of PEI was fixed at 8 mM. (B) Effect of PEI concentration on fluorescence intensity. The concentration of formaldehyde was fixed at 6 M. (C) Effect of temperature on fluorescence intensity. (D) Effect of reaction time on fluorescence intensity. Concentrations (C and D): formaldehyde (6 M), PEI (8 mM). Volumes of the final mixtures were 100 μL. (E, F) Some photos of diluted PNP solutions (0.3% v/v) that are synthesized by PEI (8 mM) and different concentrations of formaldehyde under visible light (E) and UV lamp (F).

DOI: 10.1021/acs.analchem.5b01138
Anal. Chem. 2015, 87, 8679−8686

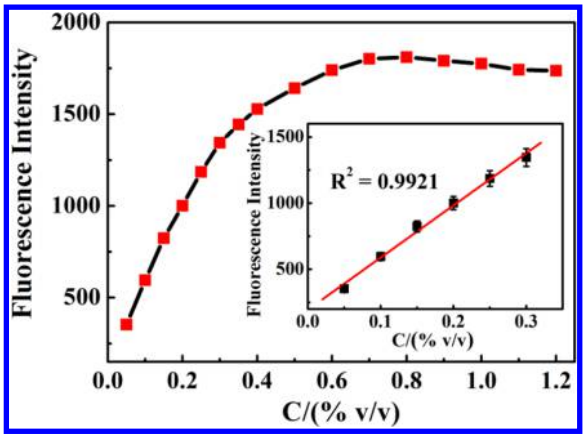

Figure 7. Relationship between fluorescence intensity and concentration of PNPs. (Inset) Linear range of 0.05−0.3% (v/v).

fluorescence intensities are positively proportional to PNP concentrations in the range 0.05−0.3% (v/v), and when the concentration of PNPs is higher than 0.3% (v/v), the fluorescence intensity increases slowly and then there is a trend to saturation. Therefore, the concentration 0.3% (v/v) PNPs was eventually chosen for obtaining absorption and fluorescence spectra. Similarly, the concentrations of PNPs prepared with other aldehydes were chosen for obtaining the mirror-imaged excitation and emission bands.

Subsequently, the conditions of gelation were optimized. At first, the concentration of PEI was fixed at 6 mM and the concentration of formaldehyde was optimized. The total volume of the mixture was 100 μL. It can be seen from Table S1 and Figure S5A that 0.36−0.96 M formaldehyde can cross-link PEI at room temperature (25 °C). Upon mixing, a gel was formed quickly. If the gel was heated at 95 °C for 25 min, all the gel became yellow (Figure S5B). In addition, when the concentration of formaldehyde was larger than 0.48 M, the gel dissolved after heating. To further investigate the molar radio of PEI to formaldehyde, the concentration of formaldehyde was fixed at 0.48 M and the amount of PEI was further studied. The concentrations of PEI solution were 4, 5, 6, 7, and 8 mM. When the concentration of PEI was in the range from 6 to 8 mM, a gel was formed. So the amounts of PEI (6 mM) and formaldehyde (0.48 M) were chosen as described in the Experimental Section. Furthermore, other aldehydes can also interact with PEI to form multicolor PNPs (Figure 8A) and gel. Under visible light, except the PNPs prepared by formaldehyde, the color of the diluted PNPs solutions (1% v/v) is almost colorless (Figure 8B), and under UV lamp illumination (365 nm), all the diluted nanoparticle solutions exhibit fluorescence with a variety of colors (Figure 8C), and then their normalized emission spectra are shown in Figure 8D. Figure 8E shows the mirror-image spectra of maximum excitation and emission bands. UV radiation has some disadvantages, including low light-penetration depth in tissues, high absorption and scattering coefficients, and its mutagenic potential.[47] However, the PNPs formed by glutaraldehyde would be a better probe for imaging in living cells. The gel before (panels A, C, E, G, I) and after (panels B, D, F, H) heating is shown in Figure S5. After heating, the colors of all the gels are darker. Specially, for propionaldehyde and butyraldehyde, their gels changed at room temperature (Figure S5E,G). When the concentration of propionaldehyde was 5.2 M, a gel formed after 30 min at ambient temperature (25 °C).

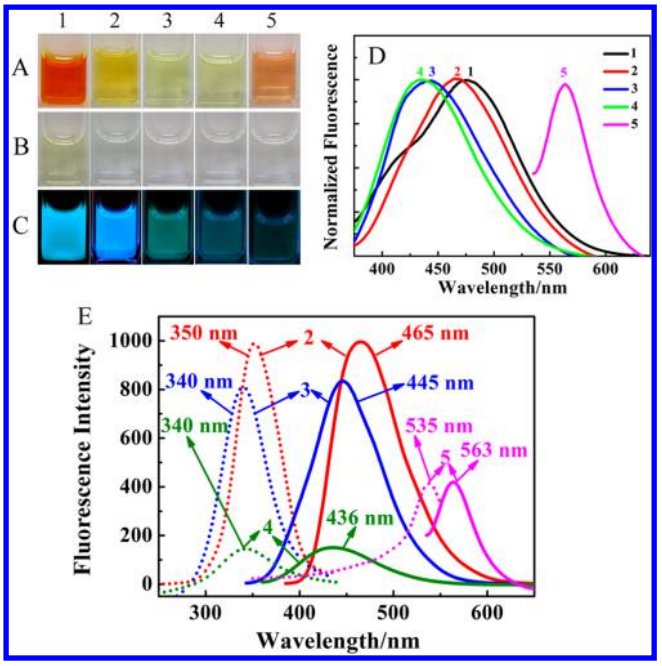

Figure 8. Photos of different PNP solutions under visible light (A) and of diluted PNP solutions (1% v/v) under visible light (B) and UV lamp (C). (D) Normalized emission spectra of different PNP solution. (E). Comparison of mirror-imaged excitation and emission bands. 1, 2, 3, 4, and 5 represent the PNP solutions synthesized by formaldehyde, acetaldehyde, propionaldehyde, butyraldehyde, and glutaraldehyde, respectively. Concentrations in panel E: 2 (1% v/v), 3 (4% v/v), 4 (5% v/v), 5 (10% v/v).

Being kept for 6 h, the gel became cloudy and bright yellow. Similarly, when the volume of butyraldehyde was 1.1 M, a gel formed after 30 min at ambient temperature.

The interesting properties of the PNPs indicate great potential for imaging in living cells. To reduce the impact of toxic formaldehyde in imaging applications, the PNPs have been used after dialysis. After 18 h of incubation, nanoparticle fluorescence in the cytoplasm (Figure 9) was clearly detected by using a confocal laser scanning microscope (CLSM). The dosage of PNPs for cell imaging could be further decreased. During the experiments, the cells showed no signal of damage. Moreover, the PNPs showed no significant photobleaching in fixed SK-N-SH cells over 5 min upon continuous excitation at 405 nm.

CONCLUSIONS

Hyperbranched PEI reacted with aldehydes and displayed multicolor PNPs and gel. The final solution shows gelation behavior at a lower concentration of aldehydes. This work may provide an inspiring strategy for naked-eye discrimination of aldehydes and visual detection of aldehydes. Highly fluorescent PNPs have been prepared by a one-step reaction without catalysts. The water-soluble nanoparticles with well-controlled size distributions exhibit high fluorescence brightness and good photostability. Fundamental properties of PNPs have been investigated, and the PNPs have been utilized as a fluorescent probe for imaging in living cells. On the other hand, our PNPs are easily surface-modified. Many other functional groups such as DNA, peptide, biotin, antibody, and drug could also be further conjugated with PNPs on their surface. Overall, our system has a brilliant future for widespread applications in chemical and biological sensing and in biological imaging.

DOI: 10.1021/acs.analchem.5b01138
Anal. Chem. 2015, 87, 8679−8686

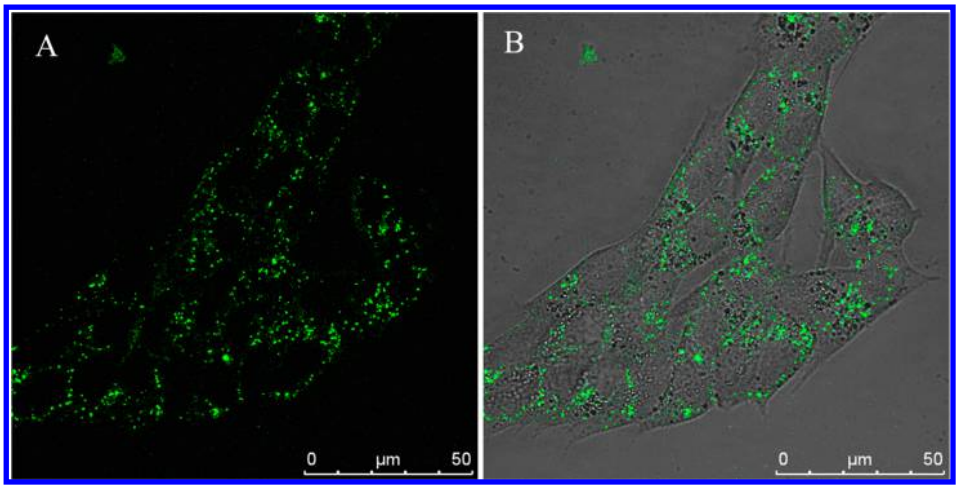

Figure 9. CLSM images of SK-N-SH cells when they were incubated with 10 μL of 20% v/v PNPs for 18 h: (A) excited with 405 nm laser; (B) overlay of fluoroscence image and bright-field image.

■ ASSOCIATED CONTENT

Supporting Information

The Supporting Information is available free of charge on the ACS Publications website at DOI: 10.1021/acs.analchem.5b01138.

Five figures showing excitation-dependent emission, comparative experiment, ^{1}H NMR of PNPs, effect of molecular weight, and photos of gels; one table listing optimization of conditions (PDF)

■ AUTHOR INFORMATION

Corresponding Authors

*Tel/fax +86 23 6825 3237; e-mail linb@swu.edu.cn (N.B.L.).
*Tel/fax +86 23 6825 3237; e-mail luohq@swu.edu.cn (H.Q.L.).

Notes

The authors declare no competing financial interest.

■ ACKNOWLEDGMENTS

We acknowledge financial support from National Natural Science Foundation of China (21273174), Municipal Science Foundation of Chongqing City (CSTC-2013jjB00002), and Fundamental Research Funds for the Central Universities of China (XDJK2014D033).

■ REFERENCES

(1) Wu, C.; Chiu, D. T. *Angew. Chem., Int. Ed.* **2013**, *52*, 3086−3109.
(2) Resch-Genger, U.; Grabolle, M.; Cavaliere-Jaricot, S.; Nitschke, R.; Nann, T. *Nat. Methods* **2008**, *5*, 763−775.
(3) Bruchez, M., Jr.; Moronne, M.; Gin, P.; Weiss, S.; Alivisatos, A. P. *Science* **1998**, *281*, 2013−2016.
(4) Chan, W. C. W.; Nie, S. M. *Science* **1998**, *281*, 2016−2018.
(5) Michalet, X.; Pinaud, F. F.; Bentolila, L. A.; Tsay, J. M.; Doose, S.; Li, J. J.; Sundaresan, G.; Wu, A. M.; Gambhir, S. S.; Weiss, S. *Science* **2005**, *307*, 538−544.
(6) Baker, S. N.; Baker, G. A. *Angew. Chem., Int. Ed.* **2010**, *49*, 6726−6744.
(7) Sun, Y. P.; Zhou, B.; Lin, Y.; Wang, W.; Fernando, K. A. S.; Pathak, P.; Meziani, M. J.; Harruff, B. A.; Wang, X.; Wang, H. F.; Luo, P. J. G.; Yang, H.; Kose, M. E.; Chen, B. L.; Veca, L. M.; Xie, S. Y. *J. Am. Chem. Soc.* **2006**, *128*, 7756−7757.
(8) He, Y.; Zhong, Y. L.; Peng, F.; Wei, X. P.; Su, Y. Y.; Lu, Y. M.; Su, S.; Gu, W.; Liao, L. S.; Lee, S. T. *J. Am. Chem. Soc.* **2011**, *133*, 14192−14195.
(9) Warner, J. H.; Hoshino, A.; Yamamoto, K.; Tilley, R. D. *Angew. Chem., Int. Ed.* **2005**, *44*, 4550−4554.
(10) Jiang, H.; Taranekar, P.; Reynolds, J. R.; Schanze, K. S. *Angew. Chem., Int. Ed.* **2009**, *48*, 4300−4316.
(11) Feng, F.; He, F.; An, L.; Wang, S.; Li, Y.; Zhu, D. *Adv. Mater.* **2008**, *20*, 2959−2964.
(12) Duan, X. R.; Liu, L. B.; Feng, F. D.; Wang, S. *Acc. Chem. Res.* **2010**, *43*, 260−270.
(13) Feng, X.; Liu, L.; Wang, S.; Zhu, D. *Chem. Soc. Rev.* **2010**, *39*, 2411−2419.
(14) McQuade, D. T.; Pullen, A. E.; Swager, T. M. *Chem. Rev.* **2000**, *100*, 2537−2574.
(15) Thomas, S. W.; Joly, G. D.; Swager, T. M. *Chem. Rev.* **2007**, *107*, 1339−1386.
(16) An, L. L.; Wang, S. *Chem. - Asian J.* **2009**, *4*, 1196−1206.
(17) Pu, K. Y.; Liu, B. *Adv. Funct. Mater.* **2011**, *21*, 3408−3423.
(18) Zhu, C. L.; Liu, L. B.; Yang, Q.; Lv, F. T.; Wang, S. *Chem. Rev.* **2012**, *112*, 4687−4735.
(19) Feng, L.; Zhu, C.; Yuan, H.; Liu, L.; Lv, F.; Wang, S. *Chem. Soc. Rev.* **2013**, *42*, 6620−6633.
(20) Tuncel, D.; Demir, H. V. *Nanoscale* **2010**, *2*, 484−494.
(21) Wu, C. F.; Szymanski, C.; Cain, Z.; McNeill, J. *J. Am. Chem. Soc.* **2007**, *129*, 12904−12905.
(22) Feng, L.; Liu, L.; Lv, F.; Bazan, G. C.; Wang, S. *Adv. Mater.* **2014**, *26*, 3926−3930.
(23) Wu, C.; Bull, B.; Szymanski, C.; Christensen, K.; McNeill, J. *ACS Nano* **2008**, *2*, 2415−2423.
(24) Wu, C.; Schneider, T.; Zeigler, M.; Yu, J.; Schiro, P. G.; Burnham, D. R.; McNeill, J. D.; Chiu, D. T. *J. Am. Chem. Soc.* **2010**, *132*, 15410−15417.
(25) Kietzke, T.; Neher, D.; Landfester, K.; Montenegro, R.; Guntner, R.; Scherf, U. *Nat. Mater.* **2003**, *2*, 408−412.
(26) Kaeser, A.; Schenning, A. P. *Adv. Mater.* **2010**, *22*, 2985−2997.
(27) Pecher, J.; Mecking, S. *Chem. Rev.* **2010**, *110*, 6260−6279.
(28) Lee, W. I.; Bae, Y.; Bard, A. J. *J. Am. Chem. Soc.* **2004**, *126*, 8358−8359.
(29) Wang, D.; Imae, T. *J. Am. Chem. Soc.* **2004**, *126*, 13204−13205.
(30) Wu, D. C.; Liu, Y.; He, C. B.; Goh, S. H. *Macromolecules* **2005**, *38*, 9906−9909.
(31) Lei, Y.; Segura, T. *Biomaterials* **2009**, *30*, 254−265.
(32) Glodde, M.; Sirsi, S. R.; Lutz, G. J. *Biomacromolecules* **2006**, *7*, 347−356.
(33) Pastor-Pérez, L.; Chen, Y.; Shen, Z.; Lahoz, A.; Stiriba, S. E. *Macromol. Rapid Commun.* **2007**, *28*, 1404−1409.

DOI: 10.1021/acs.analchem.5b01138
Anal. Chem. 2015, 87, 8679−8686

(34) Lee, K.; Choi, S.; Yang, C.; Wu, H. C.; Yu, J. *Chem. Commun.* **2013**, *49*, 3028−3030.
(35) Liu, M.; Zhang, X.; Yang, B.; Deng, F.; Ji, J.; Yang, Y.; Huang, Z.; Zhang, X.; Wei, Y. *RSC Adv.* **2014**, *4*, 22294−22298.
(36) Pu, K.; Shuhendler, A. J.; Jokerst, J. V.; Mei, J.; Gambhir, S. S.; Bao, Z.; Rao, J. *Nat. Nanotechnol.* **2014**, *9*, 233−239.
(37) Rolfe, B. E.; Blakey, I.; Squires, O.; Peng, H.; Boase, N. R.; Alexander, C.; Parsons, P. G.; Boyle, G. M.; Whittaker, A. K.; Thurecht, K. J. *J. Am. Chem. Soc.* **2014**, *136*, 2413−2419.
(38) Sun, Y. P.; Zhou, B.; Lin, Y.; Wang, W.; Fernando, K. A. S.; Pathak, P.; Meziani, M. J.; Harruff, B. A.; Wang, X.; Wang, H.; Luo, P. G.; Yang, H.; Kose, M. E.; Chen, B.; Veca, L. M.; Xie, S. Y. *J. Am. Chem. Soc.* **2006**, *128*, 7756−7757.
(39) Zhang, X.; Yu, J.; Wu, C.; Jin, Y.; Rong, Y.; Ye, F.; Chiu, D. T. *ACS Nano* **2012**, *6*, 5429−5439.
(40) Zhang, Q. T.; Tour, J. M. *J. Am. Chem. Soc.* **1998**, *120*, 5355−5362.
(41) Yoshihara, T.; Druzhinin, S. I.; Zachariasse, K. A. *J. Am. Chem. Soc.* **2004**, *126*, 8535−8539.
(42) Qu, F.; Li, N. B.; Luo, H. Q. *Langmuir* **2013**, *29*, 1199−1205.
(43) Xia, T.; Kovochich, M.; Liong, M.; Meng, H.; Kabehie, S.; George, S.; Zink, J. I.; Nel, A. E. *ACS Nano* **2009**, *3*, 3273−3286.
(44) Dong, Y. Q.; Wang, R. X.; Li, H.; Shao, J. Y.; Chi, Y. W.; Lin, X. M.; Chen, G. N. *Carbon* **2012**, *50*, 2810−2815.
(45) Mui, C.; Han, J. H.; Wang, G. T.; Musgrave, C. B.; Bent, S. F. *J. Am. Chem. Soc.* **2002**, *124*, 4027−4038.
(46) Tsuji, K.; Shibuya, K. *J. Phys. Chem. A* **2009**, *113*, 9945−9951.
(47) Jayakumar, M. K.; Idris, N. M.; Zhang, Y. *Proc. Natl. Acad. Sci. U. S. A.* **2012**, *109*, 8483−8488.

DOI: 10.1021/acs.analchem.5b01138
Anal. Chem. 2015, 87, 8679−8686